

Blind parameter estimation of pseudo-random binary code-linear frequency modulation signal based on Duffing oscillator at low SNR

Ke Wang(王珂), Xiaopeng Yan(闫晓鹏), Ze Li(李泽), Xinhong Hao(郝新红), Honghai Yu(于洪海)
Citation: Chin. Phys. B, 2021, 30 (**5**): 050708. DOI: 10.1088/1674-1056/abd75f
Journal homepage: http://cpb.iphy.ac.cn; http://iopscience.iop.org/cpb

What follows is a list of articles you may be interested in

Design and FPGA implementation of multi-wing chaotic switched systems based on a quadratic transformation

Qing-Yu Shi(石擎宇), Xia Huang(黄霞), Fang Yuan(袁方), and Yu-Xia Li(李玉霞)
Chin. Phys. B, 2021, 30 (**2**): 020507. DOI: 10.1088/1674-1056/abd74c

A multi-directional controllable multi-scroll conservative chaos generator: Modelling, analysis, and FPGA implementation

En-Zeng Dong(董恩增), Rong-Hao Li(李荣昊), and Sheng-Zhi Du(杜升之)
Chin. Phys. B, 2021, 30 (**2**): 020505. DOI: 10.1088/1674-1056/abc239

Chaotic signal denoising algorithm based on sparse decomposition

Jin-Wang Huang(黄锦旺), Shan-Xiang Lv(吕善翔), Zu-Sheng Zhang(张足生), Hua-Qiang Yuan(袁华强)
Chin. Phys. B, 2020, 29 (**6**): 060505. DOI: 10.1088/1674-1056/ab8a3b

Weak wide-band signal detection method based on small-scale periodic state of Duffing oscillator

Jian Hou(侯健), Xiao-peng Yan(闫晓鹏), Ping Li(栗苹), Xin-hong Hao(郝新红)
Chin. Phys. B, 2018, 27 (**3**): 030702. DOI: 10.1088/1674-1056/27/3/030702

Fast filtering algorithm based on vibration systems and neural information exchange and its application to micro motion robot

Gao Wa, Zha Fu-Sheng, Song Bao-Yu, Li Man-Tian
Chin. Phys. B, 2014, 23 (**1**): 010701. DOI: 10.1088/1674-1056/23/1/010701

Blind parameter estimation of pseudo-random binary code-linear frequency modulation signal based on Duffing oscillator at low SNR*

Ke Wang(王珂), Xiaopeng Yan(闫晓鹏)†, Ze Li(李泽), Xinhong Hao(郝新红), and Honghai Yu(于洪海)

Science and Technology on Electromechanical Dynamic Control Laboratory, School of Mechatronical Engineering, Beijing Institute of Technology, Beijing 100081, *China*

(Received 23 October 2020; revised manuscript received 21 December 2020; accepted manuscript online 30 December 2020)

Conventional parameter estimation methods for pseudo-random binary code-linear frequency modulation (PRBC-LFM) signals require prior knowledge, are computationally complex, and exhibit poor performance at low signal-to-noise ratios (SNRs). To overcome these problems, a blind parameter estimation method based on a Duffing oscillator array is proposed. A new relationship formula among the state of the Duffing oscillator, the pseudo-random sequence of the PRBC-LFM signal, and the frequency difference between the PRBC-LFM signal and the periodic driving force signal of the Duffing oscillator is derived, providing the theoretical basis for blind parameter estimation. Methods based on amplitude method, short-time Fourier transform method, and power spectrum entropy method are used to binarize the output of the Duffing oscillator array, and their performance is compared. The pseudo-random sequence is estimated using Duffing oscillator array synchronization, and the carrier frequency parameters are obtained by the relational expressions and characteristics of the difference frequency. Simulation results show that this blind estimation method overcomes limitations in prior knowledge and maintains good parameter estimation performance up to an SNR of −35 dB.

Keywords: Duffing oscillator, pseudo-random binary code-linear frequency modulation (PRBC-LFM) signal, blind parameter estimation, low signal-to-noise ratio (SNR)

PACS: 07.50.Qx, 05.45.−a **DOI:** 10.1088/1674-1056/abd75f

1. Introduction

Parameter estimation plays a significant role in the signal analysis process of both civilian and military communications, and can be used to intercept information or implement jamming in non-cooperative communication.[1,2] Pseudo-random binary code-linear frequency modulation (PRBC-LFM) signals combine the characteristics of PRBC and LFM, resulting in good measurement accuracy of distance and speed, strong anti-interference performance, and low interception probability. At present, these composite signals are used in a variety of areas such as radar and subminiature detectors.[3] Therefore, it is important to study the parameter estimation algorithm for PRBC-LFM signals in modern electronic intelligence reconnaissance.

Conventional parameter estimation techniques for PRBC-LFM signals typically require some prior knowledge. Li *et al.*[4] used the method of least squares to eliminate the pseudo-random binary code, and then processed the resulting LFM signal by fast linear demodulation. However, this approach requires the pseudo-code width to be known. In other research,[5,6] the time difference of arrival was estimated by a cyclic spectral method, although the code width and carrier frequency were known in advance. Some techniques place high requirements on the signal itself. For instance, Refs. [7,8] proposed a spectrum correlation method, but this only achieves satisfactory parameter estimation performance when the frequency modulation bandwidth is greater than the ratio of the encoding number to the pulse width. Other estimation techniques have high computational complexity. Methods have been proposed in Refs. [9–11] based on the smoothed pseudo Wigner distribution (SPWVD), spectrogram and the generalized time-frequency representation of Zhao, Atlas, and Marks (ZAM-GTFR) respectively, to extract characteristics related to the carrier frequency, coefficient of frequency modulation, and pseudo-code parameter. This time-frequency analysis incurs a heavy computational load. In Ref. [12], the fractional Fourier transform (FRFT) was used to estimate the parameters of the PRBC-LFM signal, resulting in improved noise immunity. However, this approach is relatively slow because FRFT needs to conduct a two-dimensional search. He *et al.*[13] used the discrete polynomial phase transformation (DPT) and spectrum shift to complete the blind estimation of signals, but the accuracy was negatively affected by the complexity of the procedure. In addition, all of the above studies require the signal-to-noise ratio (SNR) to be above 0 dB for effective performance. Therefore, research on the parameter estimation of PRBC-LFM signals is generally faced with the problems of requiring some prior knowledge, computational complexity, and high SNR requirements. In particular, in complex electromagnetic environments, achieving better parame-

*Project supported by the National Natural Science Foundation of China (Grant Nos. 61973037 and 61673066).

†Corresponding author. E-mail: yanxiaopeng@bit.edu.cn

© 2021 Chinese Physical Society and IOP Publishing Ltd

ter estimation performance at low SNRs is an urgent problem. For these reasons, finding out a new blind parameter estimation method with fewer SNR requirements and less computational complexity, as well as without prior knowledge, is of great importance.

Since the 1970s, the Duffing oscillator has enjoyed widespread application in the field of weak signal detection due to its sensitivity to periodic signals and immunity to noise,[14] attracting many scholars studying its basic characteristics and practical application.[15–20] Wang *et al.*[21] examined the intermittent chaotic state, which enhanced the practicality of weak signal detection in chaotic systems. A method whereby a chaotic oscillator array was used to detect weak signals of unknown frequency was also described. Costa *et al.*[22] used the Duffing oscillator array composed of five oscillators to enhance the response of each oscillator through the correlation with the reference signal, and presented a time-frequency description of the chirp signal for SNR as low as −17 dB. This method outperformed the traditional time-frequency analysis. References [23,24] estimated the PRBC signal with a known carrier frequency. However, under non-cooperative conditions, the carrier frequency of the pseudo-code phase modulation signal is usually unknown. These methods cannot generally be applied to PRBC-LFM signals, which have a changing carrier frequency. To date, there has been little research on the parameter estimation of PRBC-LFM signals based on the Duffing oscillator, so this is an interesting avenue for further study.

In this paper, a weak signal detection system is established based on the Duffing oscillator to estimate the phase code and carrier frequency of PRBC-LFM signals. The relationship among the output state of the Duffing oscillator excited by a PRBC-LFM signal, the difference frequency, and the phase code is presented. The amplitude (AP) method, short-time Fourier transform (STFT) method, and power spectrum entropy (PSE) method are used to identify different states of the Duffing oscillator. Then, Duffing oscillator array synchronization is used to estimate the pseudo-random sequence. Finally, carrier frequency parameters such as the modulation period, modulation coefficient, initial frequency, and termination frequency of the PRBC-LFM signal are obtained according to the above relationship and the characteristics of the difference frequency in the detection system. This blind parameter estimation method is simulated under different SNR conditions.

The remainder of this paper is organized as follows. The next section introduces the weak signal detection system based on the Duffing oscillator estimated by the standard sinusoidal signal and PRBC-LFM signal. In Section 3, the associated relational expression is established, Duffing oscillator array synchronization is used to estimate the phase code, and then the carrier frequency is estimated according to the characteristics of the difference frequencies. Section 4 shows the simulation experiment results based on the Duffing oscillator method compared with the SPWVD and FRFT methods. Finally, the conclusions to this study are presented in Section 5.

2. Weak signal detection system based on Duffing oscillator

2.1. Traditional Duffing oscillator system

The traditional Duffing oscillator system is excited by a standard sinusoidal signal, which can be expressed as

$$\begin{cases} \dot{x} = \omega y, \\ \dot{y} = \omega\big(-ky + ax - bx^3 + F_{\mathrm{r}}\cos(\omega_{\mathrm{d}} t) \\ \qquad + A\cos(\omega_0 t + \varphi_0) + n(t)\big), \end{cases} \tag{1}$$

where x is the displacement, k is the damping coefficient, and $-ax(t) + bx^3(t)$ is the nonlinear restoring force. According to previous researches, the Duffing oscillator system has a good chaotic state when $k = 0.5$, $a = b = 1$.[25,26] $F_{\mathrm{r}}\cos(\omega_{\mathrm{d}} t)$ is the periodic driving force signal of the Duffing oscillator. $A\cos(\omega_0 t + \varphi_0)$ is the to-be-detected signal, and $n(t)$ is the stochastic disturbance, which is Gaussian white noise in this study.

There is a critical threshold F_{c} in the Duffing oscillator system. When there is no signal to be detected, if $F_{\mathrm{r}} \le F_{\mathrm{c}}$, the system will be in a chaotic state; if $F_{\mathrm{r}} > F_{\mathrm{c}}$, the system will be in a large-scale periodic state. Adding the to-be-detected signal when $F_{\mathrm{r}} = F_{\mathrm{c}}$ results in two situations. First, $|\Delta\omega| = |\omega_{\mathrm{d}} - \omega_0|$ denotes the difference frequency of the to-be-detected signal and the periodic driving force signal of the Duffing oscillator. If $\Delta\omega = 0$, the system will transform from a chaotic state to a large-scale periodic state; if $\Delta\omega \neq 0$, the system will be converted to an intermittent chaotic state. If $|\Delta\omega \le 0.03\omega_{\mathrm{d}}|$, the intermittent chaotic state can be maintained regularly and stably. When $\Delta\omega$ exceeds this range, the rule governing the intermittent chaotic state may be broken due to the insufficient maintenance time of the equivalent policy force.[21] Figure 1 illustrates the regular intermittent chaotic state of a traditional Duffing oscillator excited by a sinusoidal signal. Here, we set $\omega_{\mathrm{d}} = 2\pi \times 100$ MHz, $\Delta\omega = 2\pi \times 3$ MHz, $F_{\mathrm{r}} = 0.826$, $A = 0.1$, and $\varphi = 0$.

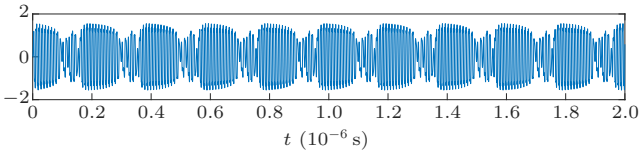


Fig. 1. Output time domain waveform of the Duffing oscillator excited by a sinusoidal signal.

2.2. PRBC-LFM signal

The PRBC signal can be expressed as

$$P(t)=\frac{1}{\sqrt{NP}}\sum_{m=0}^{N-1}\sum_{n=0}^{P-1}C_i\mu(t-nT_{r1}-mT_{r2})e^{j\varphi_i}, \tag{2}$$

where $\mu(t)=1/\sqrt{T_p}\text{rect}(t/T_p)$, and $\text{rect}(t/T_p)=\begin{cases}1, 0\le t<T_p,\\ 0, \quad \text{else},\end{cases}$ is the unit pulse with a width of T_p, P is the number of pulses, T_{r1} is the pulse repetition period, N is the number of repetition periods of the pseudo-random code, $T_{r2}=PT_{r1}$ is the repetition period of the pseudo-random code, $C_i=\{+1,-1\}$, and $\varphi_i=\{0,\pi\}$ represents the phase code with $\varphi_i=\begin{cases}0, & P(t)=1,\\ \pi, & P(t)=-1.\end{cases}$ If $T_{r1}>T_p$, the PRBC signal is a pulse system; if $T_{r1}=T_p$, it is a continuous wave system. This paper considers only the latter case.

The sawtooth linear frequency modulation signal can be expressed as

$$L(t)=\frac{1}{\sqrt{N}}\sum_{m=0}^{N}s_{LFM}(t-mT_M), \tag{3}$$

where

$$s_{LFM}(t)=\begin{cases}e^{j\left[\omega_0 t+\pi k_f t^2+\varphi_0\right]}, & 0<t<PT_p,\\ 0, & \text{else},\end{cases}$$

ω_0 is the initial carrier frequency, and φ_0 is the initial phase. Taking the sawtooth wave as an example, k_f is the modulation coefficient with $k_f=\Delta F_M/T_M$, ΔF_M is the modulation bias, T_M is the modulation period, and M is the number of modulation periods.

The PRBC-LFM composite signal can be regarded as the product of the PRBC signal and the LFM signal. In the case of one modulation period, the PRBC-LFM signal can be simplified to:

$$s(t)=A\cos\left(\omega_0 t+\pi k_f t^2+\varphi_0+\varphi_i\right) \tag{4}$$

where A is the amplitude. As shown in Eq. (4), we need to estimate three parameters of the PRBC-LFM signal, namely the initial frequency, modulation coefficient, and phase code.

If we input the PRBC-LFM signal into the Duffing oscillator system, the Duffing oscillator can be written as

$$\begin{cases}\dot{x}=\omega y,\\ \dot{y}=\omega(-0.5y+x-x^3+F_r\cos(\omega_d t)\\ \quad +A\cos((\omega_0+\pi k_f t)t+\varphi_0+\varphi_i)+n(t)),\end{cases} \tag{5}$$

where $\Delta\omega=\omega_d-(\omega_0+\pi k_f t)$. As for the sinusoidal signal, we set $F_r=F_c$, so that when $0<|\Delta\omega|\le 0.03\omega$, the Duffing oscillator excited by the PRBC-LFM signal will be converted to the regular intermittent chaotic state. However, although there is a certain regularity, the intermittent chaotic state of the PRBC-LFM signal is different from the sinusoidal signal, because of the constantly changing phase and frequency. The time domain waveform is shown in Fig. 2. Like the sinusoidal signal, we also fix $\omega_d=2\pi\times 100$ MHz, $\omega=2\pi\times 100$ MHz, $k_f=3/(1\times 10^{-7})$ MHz/s$=3\times 10^7$ MHz/s, $F_r=0.826$, $A=0.1$, and $\varphi_0=0$.

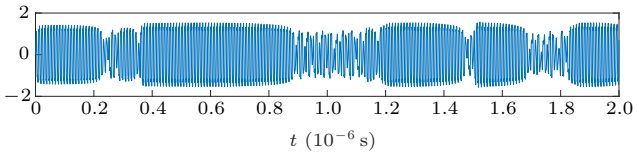


Fig. 2. Output time domain waveform of the Duffing oscillator excited by a PRBC-LFM signal.

3. Parameter estimation of PRBC-LFM signal based on duffing oscillator array

3.1. Relationship among functions in duffing oscillator system excited by PRBC-LFM signal

To determine the rule governing the intermittent chaotic state of the Duffing oscillator stimulated by the PRBC-LFM signal, the output signal needs to be further analyzed. As shown in Eq. (5), the equivalent periodic driving force signal can be represented as $F_e\cos(\omega_d t+\theta)$ after inputting the PRBC-LFM signal, where

$$F_e(t)=\sqrt{F_r^2+2F_rA\cos\left(\Delta\omega t+\varphi(t)\right)+A^2}, \tag{6}$$

$$\theta(t)=\arctan\left[\frac{A\sin\left(\Delta\omega t+\varphi(t)\right)}{F_r+A\cos\left(\Delta\omega t+\varphi(t)\right)}\right], \tag{7}$$

in which $\varphi(t)=\varphi_0+\varphi_i$, $F_r=F_c$, and $A\ll F_r$ because the to-be-detected signal is weak. Therefore, $F_e(t)$ can be written as

$$F_e(t)\approx\sqrt{F_c^2+2F_cA\cos\left(\Delta\omega t+\varphi(t)\right)}. \tag{8}$$

According to Eq. (8), we have

$$\text{sgn}(F_e(t)-F_c)=\text{sgn}\left(\cos\left(\Delta\omega t+\varphi(t)\right)\right). \tag{9}$$

In this eqnarray, sgn(number) represents the sign function: if number >0, sgn $=1$; if number $=0$, sgn $=0$; if number <0, sgn $=-1$. The relationship among the sign function $\text{sgn}\left(\cos\left(\Delta\omega t+\varphi(t)\right)\right)$, phase code φ_i, and time t is presented in Table 1, where $t_1=(2k\pi-\pi/2-\varphi_0)/|\Delta\omega|$, $t_2=(2k\pi+\pi/2-\varphi_0)/|\Delta\omega|$, $k=0,1,2,\ldots$

Table 1. Relational expression.

t	sgn	
	$\varphi_i=0$	$\varphi_i=\pi$
$t_1<t<t_2$	1	−1
$t_2<t<t_1+\pi/(2\|\Delta\omega\|)$	−1	1

Based on Eq. (9) and Table 1, we can see the implied regularity of the intermittent chaotic state of the Duffing oscillator stimulated by the PRBC-LFM signal. The relationship among the output signal of the Duffing oscillator, phase code φ_i, and

cosine function of the difference frequency $\cos(\Delta\omega t+\varphi_0)$ can be written as

$$\mathrm{sgn}\big(F_{\mathrm{e}}(t)-F_{\mathrm{c}}\big)=\mathrm{sgn}\big(\cos(\Delta\omega t+\varphi_0)\big)\times\cos(\varphi_i). \quad (10)$$

When the system is in the large-scale periodic state, $F_{\mathrm{e}}>F_{\mathrm{c}}$, so $\mathrm{sgn}(F_{\mathrm{e}}-F_{\mathrm{c}})=1$. When the system is in the chaotic state, $F_{\mathrm{e}}\le F_{\mathrm{c}}$, so $\mathrm{sgn}(F_{\mathrm{e}}-F_{\mathrm{c}})=-1$ or 0. Therefore, we can binarize the output state of the Duffing oscillator, $Sys(t)$, as follows:

$$Sys(t)=\begin{cases}1, & \mathrm{sgn}(F_{\mathrm{e}}(t)-F_{\mathrm{c}})=1,\\ -1, & \text{else.}\end{cases} \quad (11)$$

The cosine function of the difference frequency between the PRBC-LFM signal and the periodic driving force signal of the Duffing oscillator is also binarized as $Df(t)$

$$\begin{aligned}Df(t)&=\begin{cases}1, & \mathrm{sgn}\big(\cos(\Delta\omega t+\varphi_0)\big)=1,\\ -1, & \text{else,}\end{cases}\\ &=\begin{cases}1, & \dfrac{\left(2k\pi-\frac{\pi}{2}-\varphi_0\right)}{|\Delta\omega|}<t<\dfrac{\left(2k\pi+\frac{\pi}{2}-\varphi_0\right)}{|\Delta\omega|},\\ -1, & \text{else.}\end{cases}\end{aligned} \quad (12)$$

We can obtain a pseudo-random sequence $Pc(t)$ by binarizing the phase code of the PRBC-LFM signal:

$$Pc(t)=\begin{cases}1, & \cos(\varphi_i)=1,\\ -1, & \cos(\varphi_i)=-1.\end{cases} \quad (13)$$

After receiving the PRBC-LFM signal in the Duffing oscillator system, there is no stable intermittent chaotic period, where the state at a certain time is determined by both the phase code φ_i and the difference frequency $\Delta\omega$, that is,

$$Sys(t)=Df(t)\times Pc(t). \quad (14)$$

As $Sys(t)$, $Df(t)$, and $Pc(t)$ are binary functions taking values of only 1 and -1, the equivalent form of Eq. (14) is

$$Df(t)=Sys(t)\times Pc(t), \quad (15)$$

$$Pc(t)=Df(t)\times Sys(t). \quad (16)$$

Therefore, if any two of the three functions are known, the third one can be obtained using (Eqs. (14)–(16)).

3.2. Pseudo-random sequence estimation

When an array of several Duffing oscillators with different periodic driving force frequencies is excited by the PRBC-LFM signal, each oscillator will have a different intermittent chaotic period because of the difference in frequency. However, the oscillators are controlled by the same binary pseudo-random sequence $Pc(t)$, and so the state conversion time of the different Duffing oscillators in the array is always the same. Therefore, the moment when the numerical transformation occurs synchronously in different Duffing oscillators corresponds to the numerical transformation in $Pc(t)$. In this paper, we define this characteristic as the Duffing oscillator array synchronicity, which means $Sys(t)$ of each Duffing oscillator in the array varies with change of $Pc(t)$. $Sys(t)$ can be directly obtained by binarizing the Duffing oscillator output signal. As shown in Fig. 3, when $Sys(t)$ in any three of the four Duffing oscillators in the array changes at the same time, it corresponds to a change of $Pc(t)$. The Duffing oscillator array synchronicity can be used to estimate the pseudo-random sequence.

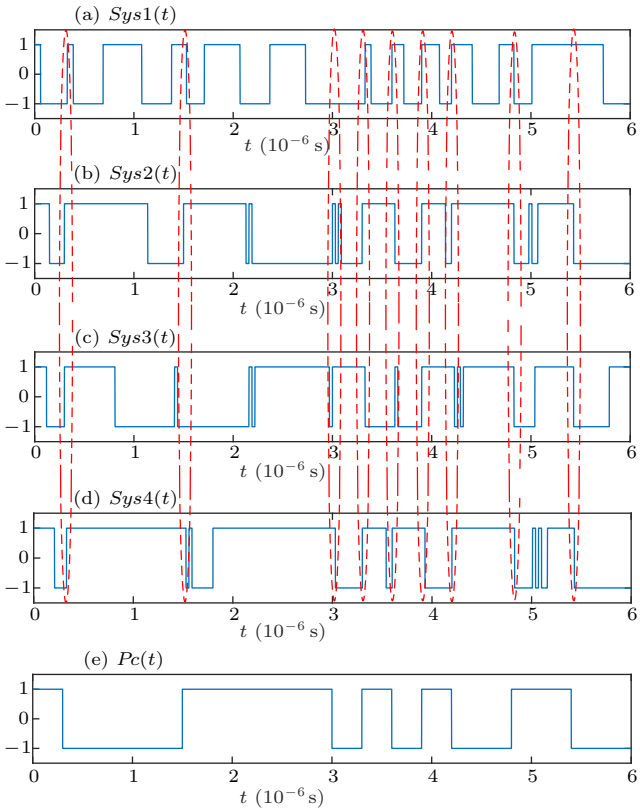


Fig. 3. Time domain diagram of $Sys(t)$ of Duffing oscillator array and $Pc(t)$.

To realize the estimation of the pseudo-random sequence $Pc(t)$ using the array synchronicity, the Duffing oscillator must first be binarized. The key to binarization is distinguishing the chaotic state from the periodic state in the intermittent chaotic state. In this paper, three binarization methods are considered: the AP method, STFT method, and PSE method. As shown in Fig. 2, the amplitudes of the chaotic and periodic states are somewhat different, so they can be distinguished according to their amplitudes, except when there is a large amount of noise or the amplitude of the signal to be measured is small. In these cases, the amplitude difference between the two states is not obvious, which may easily lead to misjudgment and affect the blind estimation. The frequencies of different states are also different, so the STFT method can be used to perform time-frequency analysis, and thus identify the states. In addition, entropy is a measure of the degree of chaos, so it can be used to distinguish the chaotic state from the periodic state. Thus,

the PSE is proposed to binarize the output of Duffing oscillators and obtain $Sys(t)$. After binarizing the Duffing oscillator's output, we can estimate the pseudo-random sequence based on the Duffing oscillator array synchronicity.

3.3. Carrier frequency estimation

After obtaining the pseudo-random sequence $Pc(t)$ by processing the array of five Duffing oscillators excited by the PRBC-LFM signal in Subsection 3.2, $Df(t)$ was determined based on Eq. (15). Since the carrier frequency of the signal to be measured is constantly changing under the control of the modulation coefficient k_f, $Df(t)$ multiplied by $Pc(t)$ and the output $Sys(t)$ of each Duffing oscillator in the array also changes continually. There are four relationships between the frequency of the Duffing oscillator periodic driving force ω_{dj} (j represents the number of oscillators) and the PRBC-LFM signal ω_0: (i) $\omega_{dj} < \omega_{0start}$, at this time, with the increase of ω_0, $\Delta\omega$ also increases gradually; (ii) $\omega_{dj} < \omega_{0end}$, where $\Delta\omega$ decreases as ω increases; (iii) $\omega_{0start} < \omega_{dj} < \omega_{0end}$, where $\Delta\omega$ first decreases, and then increases; and (iv) $\omega_{dj} = \omega_{0start}$ or $\omega_{dj} = \omega_{0end}$, where although $\Delta\omega$ increases or decreases gradually, the positive and negative values of the first or last period in the obtained difference frequency diagram vary significantly. Figure 4 illustrates $Df(t)$ in each of these cases.

In Fig. 4, the dotted red lines divide the Duffing oscillators into three periods. The change in the difference frequency in each period is the same, so the time between every pair of dotted red lines is the modulation period T_M. In the figure, the red serial numbers represent the starting period and the ending period of each oscillator, and the frequency corresponding to the red serial number i can be written as $\Delta\omega_i$. In Fig. 4(a), the time period from serial number 1 to 2 gradually decreases, which means that the frequency gradually increases, as in case (i). The initial frequency measured by oscillator 1 is $\omega_{0start1} = \omega_{d1} + \Delta\omega_1$, and the terminal frequency is $\omega_{0end1} = \omega_{d1} + \Delta\omega_2$. The time difference between 1 and -1 of the serial number 3 in Fig. 4(b) is large, after which the time period returns to normal, corresponding to case (iv), and the initial frequency obtained by oscillator 2 is equal to the periodic driving force frequency of oscillator 2. The termination frequency is $\omega_{0end2} = \omega_{d2} + \Delta\omega_4$ according to the serial number 4. In Fig. 4(c), the time period from serial number 5 to 6 first rises and then declines, satisfying the case of (iii), with an initial frequency measured by oscillator 3 of $\omega_{0start3} = \omega_{d3} - \Delta\omega_5$, and a terminal frequency of $\omega_{0end3} = \omega_{d3} + \Delta\omega_6$. At the same time, in Fig. 4(d), the time difference between 1 and -1 of serial number 8 is very different, again representing case (iv), so $\omega_{0end4} = \omega_{d4}$. According to serial number 7, the termination frequency is $\omega_{0start4} = \omega_{d4} - \Delta\omega_7$. In Fig. 4(e), the time period from serial number 9 to 10 gradually increases, so it meets the case of (ii), with an initial frequency based on oscillator 1 of $\omega_{0start5} = \omega_{d5} - \Delta\omega_9$, and a terminal frequency of $\omega_{0end5} = \omega_{d5} - \Delta\omega_{10}$.

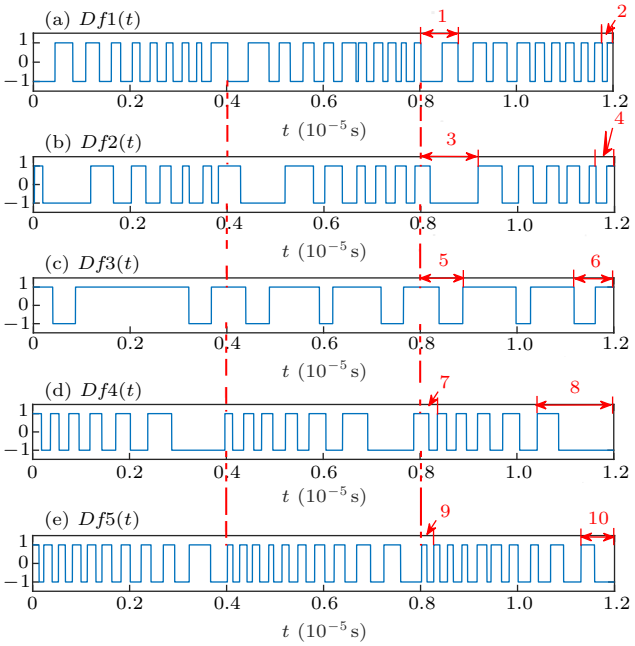


Fig. 4. Time domain diagram of $Df(t)$.

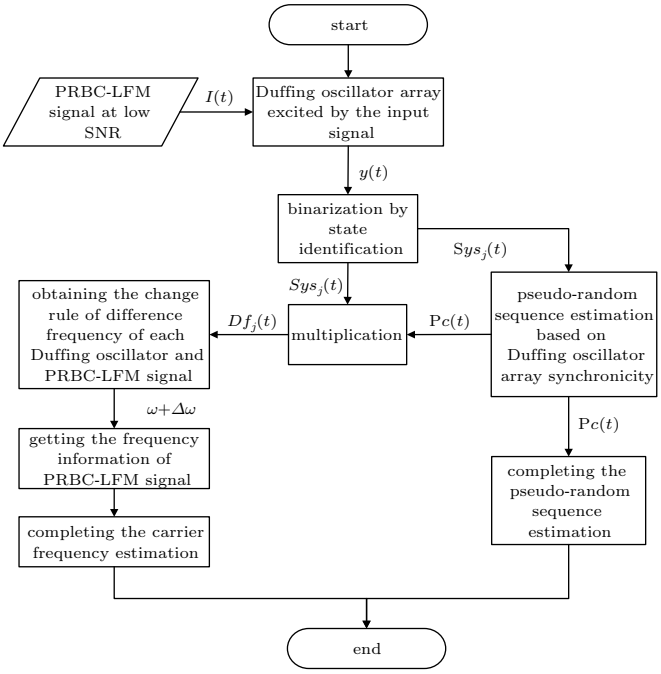


Fig. 5. Flow chart of parameter estimation method.

The average of the initial frequencies $\omega_{0starti}$ and the termination frequencies ω_{0endi} measured by the five Duffing oscillators gives the final ω_{0start} and ω_{0end}. The modulation frequency can then be written as $\Delta F_M = -(\omega_{0start} - \omega_{0end})/(2\pi)$, giving a modulation coefficient of $k_f = \Delta F_M / T_M$. A larger number of oscillators would result in higher accuracy, but with correspondingly greater computational complexity.

In summary, a flow chart of the proposed blind parameter estimation method for PRBC-LFM signal based on a Duffing oscillator array is shown in Fig. 5.

4. Simulation experiment and analysis

4.1. Pseudo-random sequence estimation simulation

We fix the amplitude of the PRBC-LFM signal to be 0.1, the initial frequency to be $\omega_{0\text{start}} = 2\pi \times 100$ MHz, the terminal frequency to be $\omega_{0\text{end}} = 2\pi \times 103$ MHz, and the pseudo-random sequence over 6×10^{-6} s to be 10000111110101001100. The frequency of the periodic driving force of the Duffing oscillator ω_{d} and the frequency of the PRBC-LFM signal ω_0 have five possible relationships: $\omega_{\text{d}} = \omega_{0\text{start}}$, $\omega_{\text{d}} < \omega_{0\text{start}}$, $\omega_{0\text{start}} < \omega_{\text{d}} < \omega_{0\text{end}}$, $\omega_{\text{d}} = \omega_{0\text{end}}$, $\omega_{\text{d}} > \omega_{0\text{end}}$. Therefore, we set up an array of five Duffing oscillators to estimate the pseudo-random sequence, and set their ω_{d} values to $2\pi \times 99$ MHz, $2\pi \times 100$ MHz, $2\pi \times 101.5$ MHz, $2\pi \times 103$ MHz, and $2\pi \times 104$ MHz, respectively.

Because of the advantages of equal spectrum, simple and convenient in mathematical processing, Gaussian white noise occupies an important position in practical application. Most of the undulating processes in radio equipment can be treated as Gaussian white noise. Many other interfering processes can be also treated as Gaussian white noise as long as their power spectrum is much wider than the passband of the system and their power spectrum density is evenly distributed in and around the passband of the system. Therefore, when detecting weak signals, the detection effect under the background of Gaussian white noise is generally analyzed. To realize signal detection under different SNRs, the variance σ^2 of the Gaussian noise is adjusted to be 0, 0.5, 5, 15.8114, and 50, respectively, corresponding to the SNR being noiseless, -20 dB, -30 dB, -35 dB and -40 dB. The time domain waveform of $Pc(t)$ is obtained based on $Sys(t)$, using the AP, STFT and PSE methods. The Duffing oscillator array synchronization is shown in Figs. 6–10.

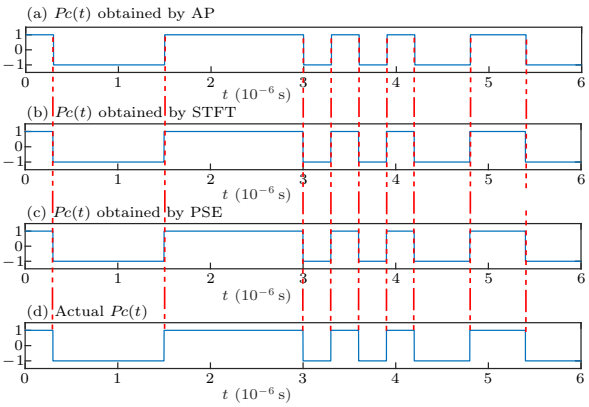


Fig. 6. $Pc(t)$ without noise.

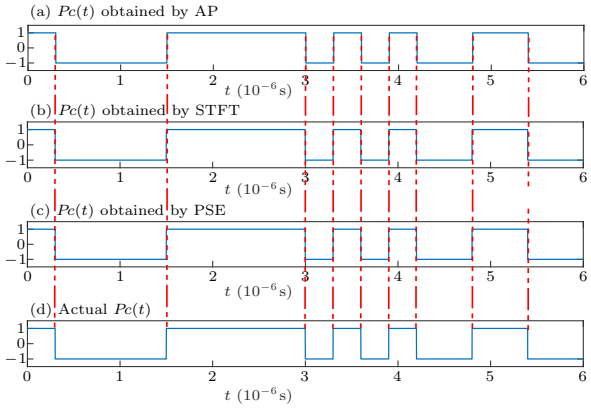


Fig. 7. $Pc(t)$ in -20 dB SNR.

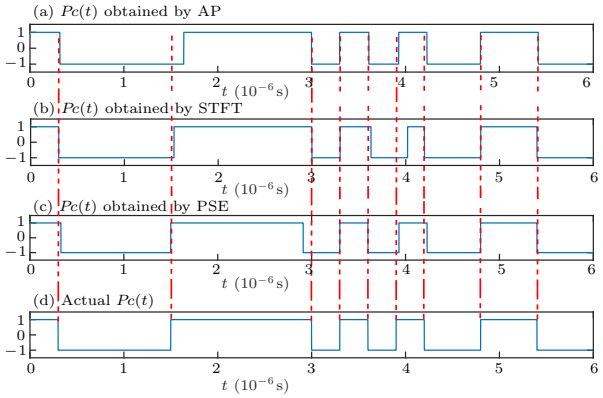


Fig. 8. $Pc(t)$ in -30 dB SNR.

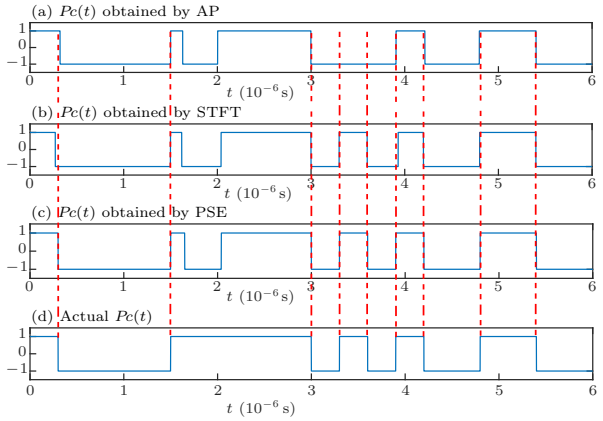


Fig. 9. $Pc(t)$ in -35 dB SNR.

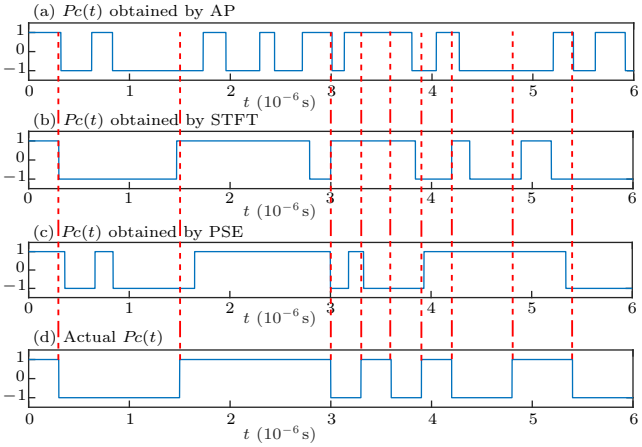


Fig. 10. $Pc(t)$ in -40 dB SNR.

Pearson's correlation coefficient is used to compare the correlation between the $Pc(t)$ obtained by each method and the actual $Pc(t)$ under different SNRs. The results are presented in Table 2. Pearson's correlation coefficient is defined as the quotient of the covariance and the standard deviation between two variables, and its formula is[27]

$$\rho_{x,y} = \frac{\mathrm{cov}(x,y)}{\sigma_x \sigma_y}. \tag{17}$$

From Figs. 6–10 and Table 2, it can be seen that all three methods give good estimation results for pseudo-random sequence estimation under an SNR of −35 dB. As the SNR decreases, the Pearson's correlation coefficients of all three methods gradually decrease. The AP method exhibits the worst anti-noise performance, with a correlation coefficient of less than 0.8 at −35 dB. The binarization method based on PSE gives an estimated pseudo-random sequence that is close to the actual sequence, providing the best anti-noise performance.

Table 2. Simulation results under different SNR.

SNR	Pearson's correlation coefficient		
	AP	STFT	PSE
without noise	1	1	1
−20 dB	1	1	1
−30 dB	0.9197	0.9402	0.9408
−35 dB	0.7758	0.8510	0.8774
−40 dB	0.2131	0.4801	0.5158

Therefore, we use the PSE method to binarize the output of the Duffing oscillator array to get $Sys(t)$. For universality, 100 experiments are conducted under each SNR. We also simulate the SPWVD method in Ref. [9] and FRFT in Ref. [12] method under different SNRs as a contrast; the conditions of these two methods are the same as the Duffing oscillator method. However, the performance of these two methods is poor under −20 dB; we only compare these three methods at −20 dB to 5 dB. The normalized root mean squared error (NRMSE) results of pseudo-code width are shown in Fig. 11. Here, the NRMSE is defined as[9–12]

$$\mathrm{NRMSE} = \frac{\sqrt{\frac{1}{N}\sum_{k=1}^{N}(x_k - x_0)^2}}{x_0}, \tag{18}$$

where x is the true value of the parameter, x_k is the estimation value of parameter, and N is the estimation time.

As shown in Fig. 11, the Duffing oscillator method proposed in this paper can estimate the pseudo-random code width more accurately under different SNRs than the SPWVD and FRFT methods. Under an SNR of −20 dB, NRMSEs based on SPWVD and FRFT methods are both more than 1.5, whereas that based on the Duffing oscillator method is only 0.0445.

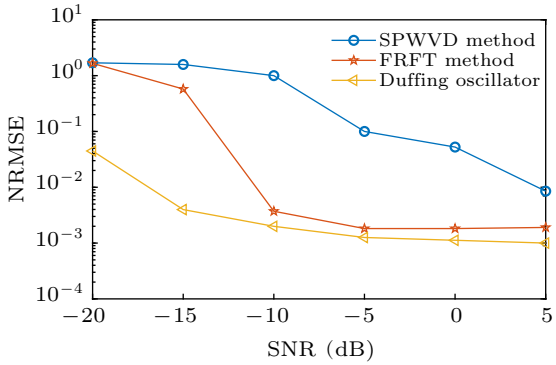


Fig. 11. NRMSE of pseudo-random code width based on three methods.

4.2. Carrier frequency estimation simulation

After obtaining the $Pc(t)$ by array synchronicity, we can determine $Df(t)$ from Eq. (15), and then estimate the carrier frequency based on the above method; 100 experiments are conducted under each SNR. Like the pseudo-code estimation simulation, we also simulate the SPWVD and FRFT methods at −20 dB to 5 dB as a contrast, which is shown in Fig. 12.

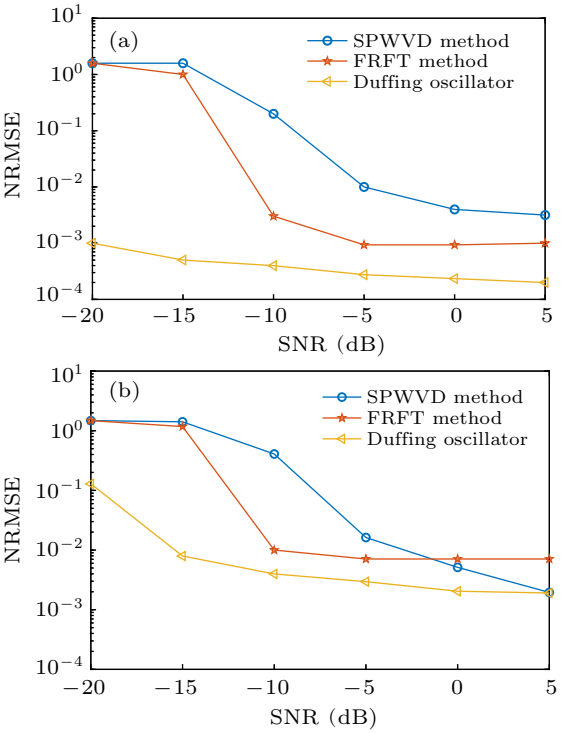


Fig. 12. NRMSE of carrier frequency based on SPWVD, FRFT and Duffing oscillator. (a) Center frequency. (b) Modulation coefficient.

In Fig. 12, the blind estimation accuracy of carrier frequency including the center frequency and modulation coefficient based on the Duffing oscillator in this paper is better than the SPWVD and FRFT methods obviously in different SNRs. In addition, the estimation of center frequency is more accurate and stable, and the estimation results have little difference at −20 dB to 5 dB.

4.3. Blind parameter estimation results

The simulation results under other SNRs are presented in Table 3. It can be seen that the center frequency estimation is more accurate than the modulation coefficient and pseudo-random code width. The NRMSE in the center frequency is only 0.107 at −40 dB, whereas those of the other two parameters are relatively large. In short, the blind parameter estimation method based on the Duffing oscillator can achieve high-precision carrier frequency and pseudo-random code estimation under an SNR of −35 dB.

Table 3. Simulation results under different SNR.

SNR	NRMSE		
	Center frequency	Modulation coefficient	Pseudo-random code width
without noise	0.000159	0.0024	0.001
−20 dB	0.000615	0.1286	0.0445
−30 dB	0.000788	0.1861	0.1
−35 dB	0.0022	0.2439	0.219
−40 dB	0.107	0.815	0.9422

In order to verify that this method can solve the problem of computational complexity, the computing time for parameter estimation of PRBC-LFM based on the Duffing oscillator under sampling number P is compared with the SPWVD and FRFT methods. All of the conditions of these three methods are the same. The simulation results are shown in Table 4. With the growth of P, the calculation time of both methods increases. However, the SPWVD method cannot compute more than the P of 3×10^4, which limits its application and anti-noise performance. Besides, the calculation time based on the Duffing oscillator is much less than that of the SPWVD and FRFT methods, especially when the value of P is large, which proves that the method presented in this paper is simpler.

Table 4. Computing time of three methods.

Method	Computer time (s)			
	$P = 3 \times 10^3$	$P = 3 \times 10^4$	$P = 3 \times 10^5$	$P = 3 \times 10^6$
SPWVD	13.3492	8594.2972	too many points to count	
FRFT	1.5811	11.3825	120.4481	2287.4263
Duffing oscillator	0.6683	2.2359	14.6609	138.987

5. Conclusions

In this study, by analyzing the output characteristics of a Duffing oscillator excited by a PRBC-LFM signal, we have derived the relationship among the output of the Duffing oscillator, pseudo-random sequence and cosine function of the difference frequency, which provides a theoretical basis for the blind estimation of PRBC-LFM signals. After binarizing the output of the Duffing oscillator array, we can estimate the pseudo-random sequence based on the Duffing oscillator array synchronicity. According to the obtained pseudo-random sequence and the multiplication relation, we obtained the binary cosine function of the difference frequency, and realized blind estimation of the carrier frequency by analyzing the time-domain diagrams of the difference frequency. Simulation results show that this method can estimate the pseudo-random sequence, carrier frequency, and frequency modulation coefficient with high accuracy, with better simulation results and less computing time than traditional methods like SPWVD and FRFT, and maintain good performance up to an SNR of −35 dB.

However, the estimation result of the carrier frequency is greatly influenced by the pseudo-random sequence, and the key is the binarization by state identification. In future work, we will attempt to find a more effective method that improves the accuracy of binarization.

References

[1] Chaudhary N I, Latif R, Raja M A and Machado J A 2020 *Appl. Math. Model.* **83** 703
[2] Shen C and Ye T 2020 *Digit. Signal Prog.* **100** 102698
[3] Wang P, Du D P, Qiu Z Y and Tang B 2014 *IEEE CSE-2014* pp. 1029–1033
[4] Zhao H C 2011 *Acta Armamentarii* **5** 543
[5] Gardner W A and Spooner C M 1993 *IEEE Trans. Commun.* **41** 231913
[6] Gardner W A and Chen C K 1992 *IEEE Trans. Signal Process* **40** 134479
[7] Xiong G, Zhao H C and Wang L J 2005 *J. Electron. Inf. Technol.* **7** 1087
[8] Zhao H C, Xiong G and Yang X N 2006 *Acta Armamentarii* **2** 258
[9] Xiong G, Yang X N and Zhao H C 2008 *J. Electron. Inf. Technol.* **30** 2115
[10] Lin J, Xiong G and Wang Z X 2006 *J. Electron. Inf. Technol.* **06** 1045
[11] Zeng X D, Tang B and Xiong Y 2012 *Chin. J. Aeronaut.* **25** 416
[12] Tang J, Zhao Y J, Zhu J D and Hu Q 2012 *Signal Process.* **09** 1271
[13] He D, Zhang T Q, Gao L and Gao H X 2012 *CISP2012* pp. 1430–1434
[14] Birx D L and Pipenberg S J 1992 *IJCNN-1992* pp. 881–888
[15] Shi H S and Li W L 2017 *Procedia Comput. Sci.* **107** 460
[16] Li C J, Xu X M, Ding Y P, Yin L Z and Dou B B 2018 *Int. J. Mod. Phys. B* **32** 1850103
[17] Akilli M and Yilmaz N 2018 *IEEE Trans. Neural Syst. Rehabil. Eng.* **26** 1918
[18] Vahedi H, Gharehpetian G B and Karrari M 2012 *IEEE Trans. Power Delivery* **27** 1973
[19] Rashtchi V and Nourazar M 2015 *Circuits, Syst. Signal Process.* **34** 3101
[20] Patel V N, Tandon N and Pandey R K 2012 *Meas.* **45** 960
[21] Wang G Y, Chen D J, Lin J Y and Chen X 1999 *IEEE Trans. Ind. Electron.* **46** 440
[22] Costa A H, Enriquezcaldera R A, Tellobello M and Bermudezgomez C R 2016 *Digit. Signal Prog.* **55** 32
[23] Zhang S and Rui G S 2012 *Int. J. Bifurcation Chaos* **22** 1250144
[24] Fu Y Q, Wu D M, Zhang L and Li X Y 2011 *Sci. China-Inf. Sci.* **54** 1274
[25] Akilli M and Yilmaz N 2018 *IEEE Trans. Neural Syst. Rehabil. Eng.* **26** 1918
[26] Rashtchi V and Nourazar M 2015 *Circuits Syst. Signal Process.* **34** 3101
[27] Rodgers J L and Nicewander W A 1988 *Am. Stat.* **42** 59